SUPPLEMENTAL FIGURES

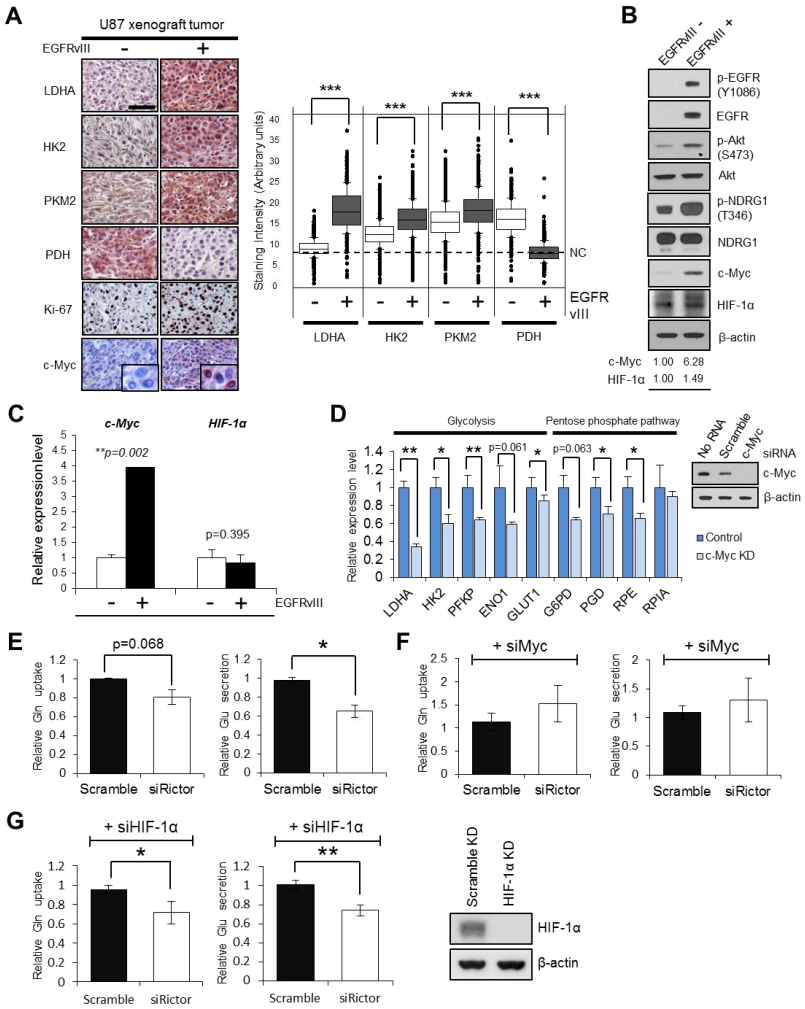

Figure S1. EGFR/mTORC2 Regulates Glycolytic Tumor Growth through c-Myc in GBM, Related to Figure 1

(A) Immunohistochemical staining of U87 and U87-EGFRvIII xenograft tumors with antibodies against a panel of glycolytic enzymes, a proliferative marker Ki-67 and c-Myc. Scale bar, 50 μm. Note that EGFRvIII signaling augments both cytoplasmic and nuclear expression of c-Myc (inset). Pyruvate dehydrogenase (PDH), whose inhibition contributes to the Warburg metabolic and malignant phenotype in cancers (McFate et al., 2008), was down-regulated in U87-EGFRvIII tumors, confirming enhanced glycolytic metabolism. NC denotes the averaged staining intensity obtained by negative control of each sample.

(B) EGFRvIII increases mTORC2 signaling (p-Akt S473 and p-NDRG1 T346) and c-Myc expression in U87 cells.

(C) mRNA levels of c-Myc and HIF-1α in U87 and U87-EGFRvIII cells.

(D) mRNA levels of glycolysis and PPP enzymes (Düvel et al., 2010) in c-Myc knockdown (KD) U87-EGFRvIII cells.

(E-G) Relative glutamine uptake and glutamate secretion which are important in tumor cell metabolism (DeBerardinis and Cheng, 2010) in control versus Rictor KD U87-EGFRvIII cells (E), combined with c-Myc KD (F) or HIF-1α KD (G). Immunoblot showing the verification of HIF-1α KD in U87-EGFRvIII cells (G).

Error bars, SEM.

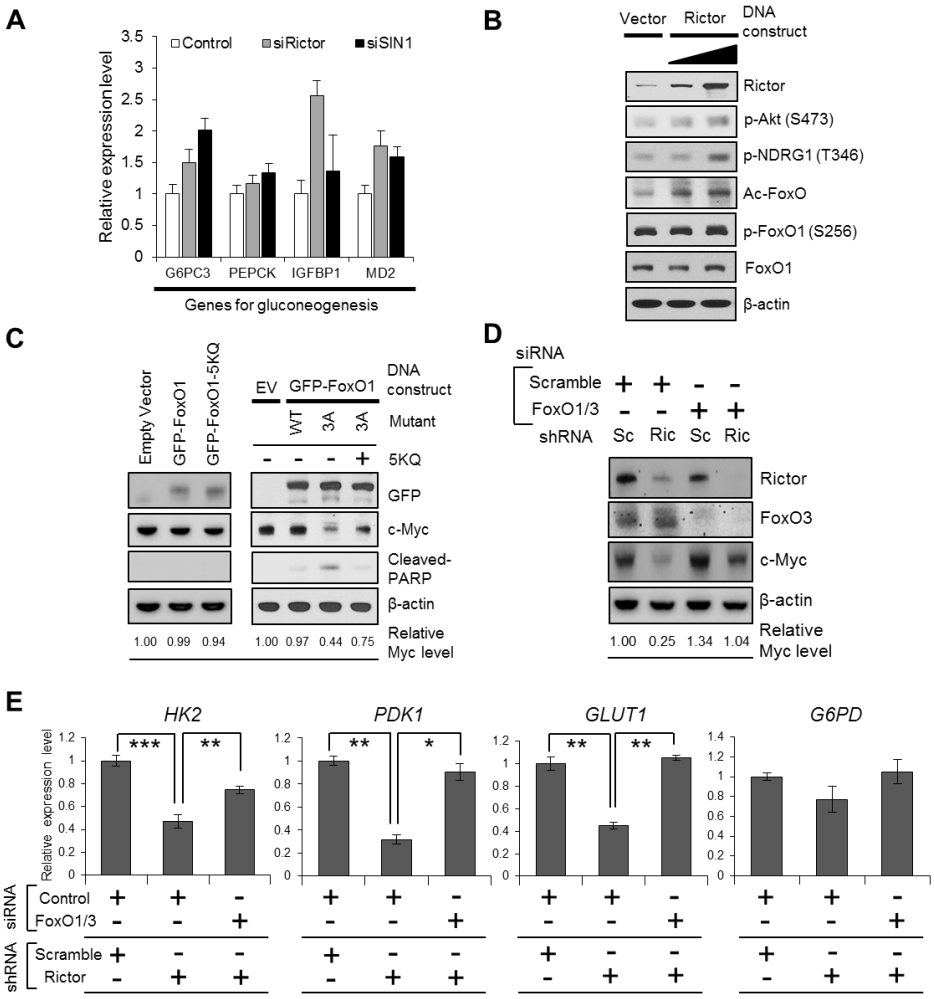

Figure S2. mTORC2 Regulates c-Myc and Glycolysis through FoxO Acetylation, Related to Figure 2

(A) Bar graph showing mRNA levels of FoxO targets including genes for gluconeogenesis (Mihaylova et al., 2011; van der Horst and Burgering, 2007) in U87-EGFRvIII cells with scramble, or mTORC2 components (Rictor and mSIN1) KD. This suggests that EGFR/mTORC2-activated tumors may suppress the new synthesis of glucose and divert the carbon source to other metabolic pathways essential for rapid cell growth.

(B) Biochemical analysis of Rictor overexpression on acetylated-FoxO in U87 cells. The acetylated FKHR (FoxO1) antibody was first validated to specifically recognize acetylated FoxO1 (MW: 52-76 kDa) in our system (data not shown).

(C) Immunoblots on the effects of wild type, 3A-, 5KQ-, or 3A-5KQ-FoxO1 on c-Myc and cleaved PARP. Note that 5KQ-mutant itself had minimal effect on c-Myc and PARP, but it displayed epistatic effect on 3A-mutant.

(D) Immunoblot assessment of c-Myc in U87-EGFRvIII cells with or without shRNA against Rictor, plus siRNA against scramble sequence or FoxO1/3.

(E) Levels of glycolytic target genes (HK2, PDK1, GLUT1) and the enzyme for PPP (G6PD) in U87-EGFRvIII with Rictor KD or Rictor and FoxO1/3 double KD cells.

Error bars, SEM.

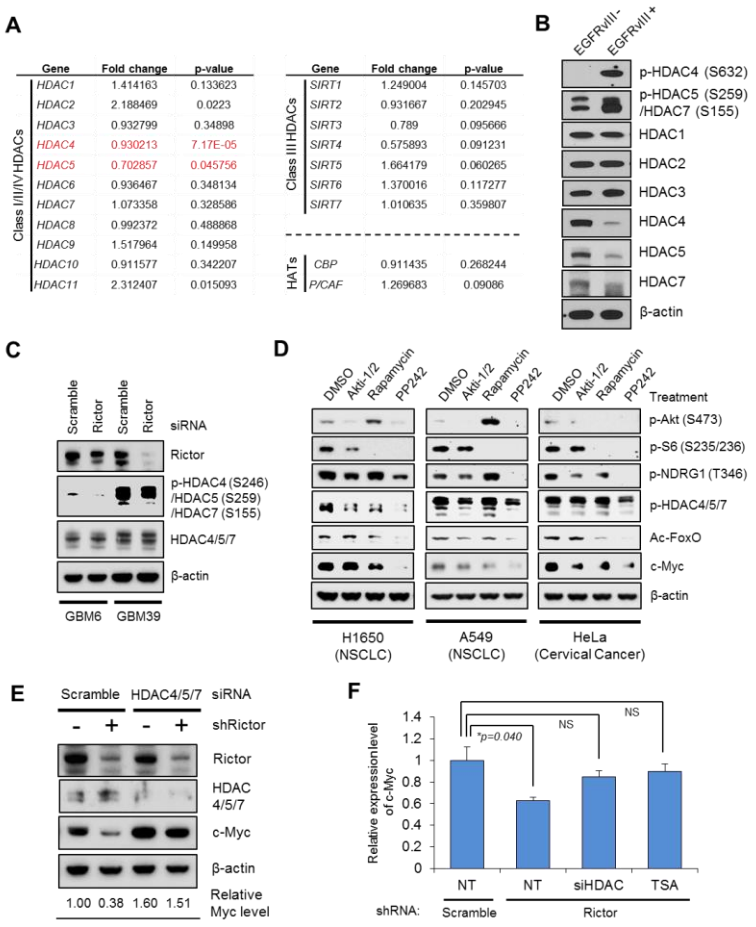

Figure S3. mTORC2 Controls FoxO Acetylation and Myc Expression via Class IIa HDACs, Related to Figure 3

(A) Expression levels of a panel of HDACs and HATs (Spiegel et al., 2012; Yang and Seto, 2007) were determined using the microarray data in U87 versus U87-EGFRvIII xenograft tumors (n = 3 in each group). Gene fold change shown is the expression level in U87-EGFRvIII tumors relative to that in parental U87 tumors.

(B) Immunoblot analysis for the status of class IIa HDACs associated with abnormal EGFR in U87 glioma cell lines.

(C) Immunoblot analysis of phosphorylated class IIa HDACs in GBM6 and GBM39 cells with scramble or Rictor KD.

(D) Assessment of phosphorylated class IIa HDACs, acetylated FoxO and c-Myc amount in H1650 (NSCLC), A549 (NSCLC) and HeLa (uterine cervical cancer) cells under pharmacologic inhibition of Akt, mTORC1 and mTORC2 for 24 h. Akti-1/2 (2.5 μM), Akt inhibitor; Rapamycin (10 nM), allosteric inhibitor of mTORC1; PP242 (2 μM), mTOR kinase inhibitor for mTORC1/2. Only PP242 treatment can suppress all three of p-HDAC, Ac-FoxO and c-Myc.

(E) Immunoblot assessment of c-Myc amount in U87-EGFRvIII cells with or without shRNA against Rictor, plus siRNA against scramble sequence or HDAC4/5/7.

(F) mRNA levels of c-Myc gene in scramble shRNA-bearing or Rictor shRNA-bearing U87-EGFRvIII cells. Myc down-regulation in Rictor KD cells can be reversed by HDAC inhibition (siRNA against class IIa HDAC (siHDAC) or Trichostatin A (TSA) treatment: 1 μM, 24 h). NT, no treatment.

Error bars, SEM.

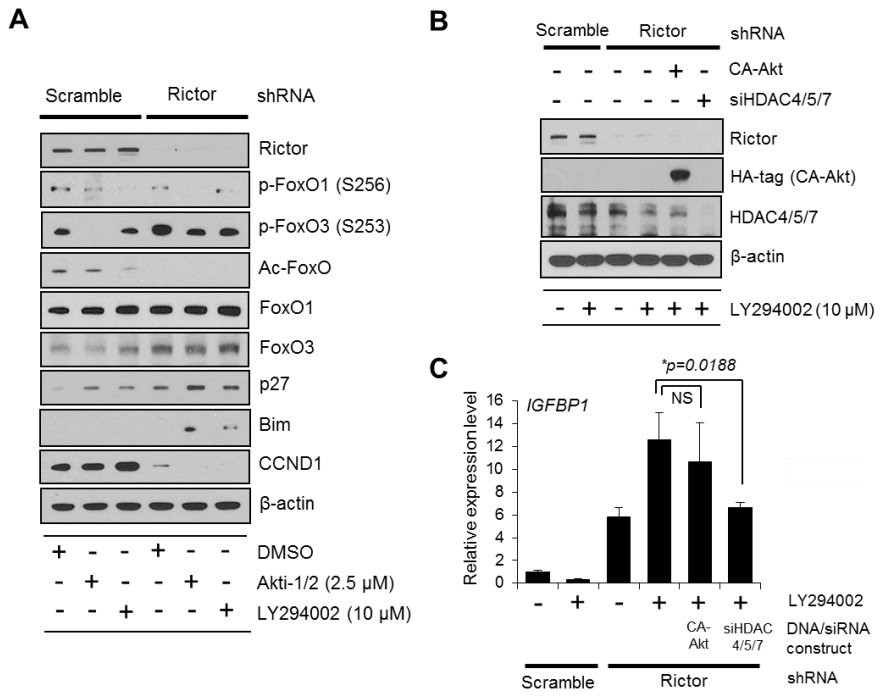

Figure S4. Resistance to PI3K and Akt Inhibitors Is Mediated by mTORC2-dependent Acetylation of FoxO and Consequent Maintenance of c-Myc, Related to Figure 5

(A) Immunoblot analysis for FoxO-targeted cell-cycle/apoptosis-related molecules (FoxO-activated genes: p27, Bim; FoxO-repressed genes: cyclin D1) in U87-EGFRvIII cells treated by PI3K/Akt inhibitors for 24 h, combined with or without Rictor KD.

(B, C) U87-EGFRvIII cells with or without Rictor KD, treated with LY294002 (for 24 h) for the assessment of FoxO recovery. The combination of Rictor and PI3K inhibition greatly restores FoxO activity, which can be slightly reversed by a constitutively active form of Akt (CA-Akt), and moderately reversed by HDAC4/5/7 KD. (B) Immunoblot for the assessment of Rictor, constitutively active Akt (HA-tag) and HDAC. (C) mRNA levels of a FoxO target gene (IGFBP1) in U87-EGFRvIII cells treated as indicated.

Error bars, SEM.

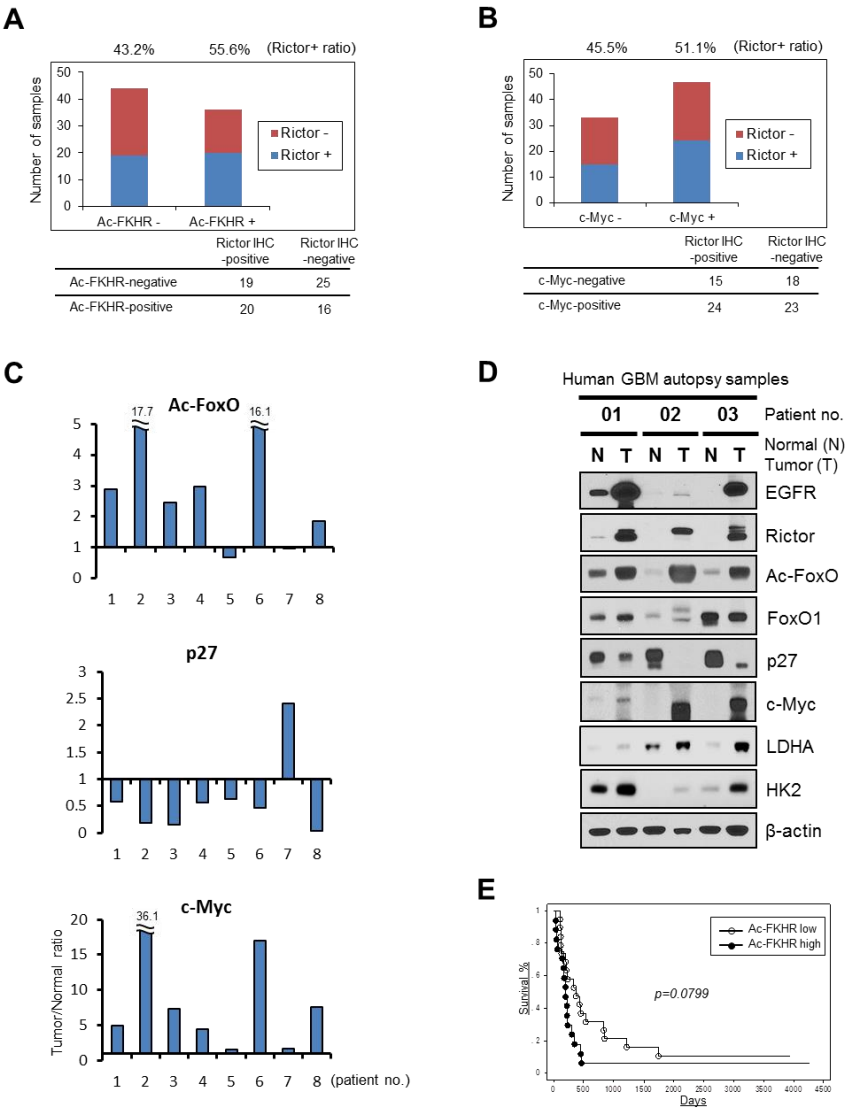

Figure S5. mTORC2/Acetylated-FoxO/c-Myc Alterations in Clinical Human GBM Samples, Related to Figure 7

(A) Bar graph showing differential association of Ac-FoxO-positve or -negative tumors with Rictor IHC positivity based on TMA.

(B) Bar graph showing differential association of c-Myc +/- tumors with Rictor immunopositivity based on TMA.

(C) Quantitative immunoblot analysis of Ac-FoxO, p27 (a FoxO target) and c-Myc, showing tumor (T) to contralateral normal brain tissue (N) ratio obtained at autopsy from 8 patients with GBM.

(D) Representative images for immunoblot analysis of autopsied GBM samples.

(E) Kaplan-Meier survival analysis for overall survival of 36 primary and secondary GBM samples classified by Ac-FoxO expression. Log-rank (Mantel-Cox) test was used to determine p values for Kaplan-Meier survival curve analyses.

SUPPLEMENTAL EXPERIMENTAL PROCEUDURES

Antibodies and Reagents

Cell signaling antibodies: EGFR, p-EGFR (Y1086), Akt, p-Akt (S473), p-S6 (S235/236), NDRG1, p-NDRG1 (T346), Raptor, Rictor, c-Myc, FoxO1, p-FoxO1 (S256), FoxO3, p-FoxO3 (S253), LDHA, HK2, PKM2, PDH, p27, Bim, Cyclin D1, HDAC4, HDAC5, HDAC7, p-HDAC4 (Ser246) / HDAC5 (Ser259) / HDAC7 (Ser155), p-HDAC4 (Ser632) / HDAC5 (Ser498) / HDAC7 (Ser486), cleaved PARP, Acetylated-Lysine, HA-tag. Santa Cruz antibodies: Ac-FKHR, HDAC4/5/7. Abcam antibodies: GFP, TBP. Sigma antibody: M2 Flag. Vector Labs antibody: Ki-67. Ambion antibody: β-actin. BD Biosciences antibody: HIF-1α. Reagents used are Akti-1/2 (EMD Chemical), LY294002 (Cell Signaling), Rapamycin (Sigma), PP242 (Chemdea), 2-Deoxy-D-glucose (Santa Cruz) and Trichostatin A (Sigma).

Cell Culture

U87-EGFRvIII isogenic GBM cell lines were obtained as described previously (Tanaka et al., 2011). Cells were cultured in DMEM (U87, U251, U138, LN229 and T98G GBM cell lines as well as A549 and HeLa cells) or RPMI-1640 (H1650 cells) supplemented with 10% FBS (Omega Scientific) in a humidified 5% CO_2 incubator at 37°C. GBM6 and GBM39 neurosphere cell lines were cultured in DMEM-F12 (Invitrogen) with N21 supplement (Millipore), Glutamax (GIBCO), EGF (Sigma), FGF (Sigma) and heparin (Sigma).

Western Blotting

Cultured cells or snap-frozen tissue samples were lysed and homogenized with a RIPA lysis buffer from Boston BioProducts (50mM Tris-HCl, 150mM NaCl, 1% NP-40, 0.5% Sodium deoxycholate, 0.1% SDS). Protein concentration of each sample was determined using the

BCA kit (Pierce) as per manufacturer's instructions. Equal amounts of protein extracts were separated by electrophoresis on 4-12% NuPAGE Bis-Tris Mini Gel (Invitrogen), and then transferred to a nitrocellulose membrane (GE Healthcare) with XCell II Blot Module (Invitrogen). The membrane was probed with various primary antibodies, followed by secondary antibodies conjugated to horseradish peroxidase. The immunoreactivity was detected with Super Signal West Pico Chemiluminescent Substrate or West Femto Trial kit (Thermo Scientific). Quantitative densitometry analysis was performed with image analysis software (ImageJ; NIH).

Immunoprecipitation (IP)

Cells were lysed in IP buffer containing 0.3% CHAPS (Fisher Scientific), 120mM NaCl, 40mM HEPES, supplemented with phosphatase inhibitor and protease inhibitor (Thermo Scientific). Cell lysates were incubated overnight at 4°C with the Dynabeads Protein A (Invitrogen)-antibody complex, washed 3 times with ice-cold PBS and analyzed by SDS-PAGE and immunoblotting.

Immunohistochemical and Immunofluorescent Staining

Immunostaining was performed as previously described (Mellinghoff et al., 2005). Slides were counterstained with hematoxylin or DAPI (Invitrogen) to visualize nuclei. Immunostained sections underwent immunohistochemical analysis in which the results were scored independently by two pathologists who were unaware of the findings of the molecular analyses. Quantitative image analysis to confirm the pathologists' scoring was also performed with Soft Imaging System software, the utility of which has been previously demonstrated for measuring drug-specific effects in GBM samples enrolled in clinical trials

with targeted agents (Mellinghoff et al., 2005; Cloughesy et al., 2008).

DNA Constructs

GFP-FoxO1, Flag-FoxO3, GFP-FoxO1-AAA, Flag-FoxO3-TM, Myc-Rictor and HA-Akt-E17K DNA plasmids were obtained from Addgene. Lentiviral shRNA vectors targeting human Rictor and scramble shRNA were also obtained from Addgene. miR-34c, miR-145, anti-miR-34c, anti-miR-145 and their negative control constructs were purchased from System Biosciences.

DNA Plasmid, siRNA and shRNA Transfection

Transfections of DNA plasmids were performed using X-tremeGENE HP (Roche) in full serum, with medium change after 24 hours, and cells were typically harvested 48 h post-transfection. Transfection of siRNA into cell lines was carried out using Lipofectamine RNAiMAX (Invitrogen) in full serum, with medium change after 24 hours. siRNAs were used at 10 nM, and cells were harvested 48 h post-transfection. Lentivirus-mediated delivery of shRNA was performed as described previously (Guo et al., 2009). Cells were infected in the presence of 6 μg/ml protamine sulfate, selected for puromycin resistance, and analyzed on the seventh day after infection.

TUNEL Assay

For TUNEL assays, cells were placed in 8-well chamber slides at 2 x 10^4 cells/well in 500 μl of growth media and then incubated for 24 hours in each condition of treatment. Apoptotic cells were evaluated with the In Situ Cell Death Detection Kit, Fluorescein following the manufacturer's protocol (Roche), and nuclei are counterstained blue by DAPI (Invitrogen).

TUNEL-positive cells were visualized with a fluorescein microscope (Nikon ECLIPSE 90i). The percentage of apoptosis was calculated as the ratio of TUNEL-positive cells out of 400 cells from each group using NIH images.

Chromatin Immunoprecipitation (ChIP)

ChIP experiment was performed using SimpleChIP^{TM} Enzymatic Chromatin IP Kit (Cell Signaling) according to the manufacturer's instruction. U87-EGFRvIII cells were transfected with GFP-N1 or GFP-FoxO1-5KR plasmids and fixed in 1% formaldehyde. Nuclear extracts were prepared with Micrococcal Nuclease digestion and following sonication. Chromatin was immunoprecipitated with anti-GFP (Abcam, ab290) at 1:50 dilution. Immunoprecipitated chromatin was washed and de-crosslinked, and purified DNA was quantified by SYBR-Green real-time quantitative PCR. Recoveries were calculated as percent of input.

Microarray Analysis

Isogenic human glioma cells U87 and U87-EGFRvIII were implanted subcutaneous (s.c.) into immunodeficient SCID/Beige mice at the AALAC-approved Animal Facility of the Division of Experimental Radiation Oncology, UCLA. U87 and U87-EGFRvIII cell lines were re-suspended at 1 x 10^6 cells/ml in PBS with Matrigel (BD Biosciences) and were implanted s.c. on opposite sides of the mouse abdomen. RNA was isolated from these xenograft tumors with TRIzol reagent (Invitrogen). For microarray analysis, RNA was DNase (Ambion) treated and amplified using the WT Expression Kit (Ambion) and WT Terminal Labeling kit (Affymetrix). Human Research Junction Arrays were obtained from Affymetrix, and labeled samples were hybridized and scanned, and gene expression was analyzed in the UCLA DNA Microarray Facility.

SUPPLEMENTAL REFERENCES

Cloughesy, T.F., Yoshimoto, K., Nghiemphu, P., Brown, K., Dang, J., Zhu, S., Hsueh, T., Chen, Y., Wang, W., Youngkin, D., et al. (2008). Antitumor activity of rapamycin in a Phase I trial for patients with recurrent PTENdeficient glioblastoma. PLoS Med. 5, e8.

DeBerardinis, R.J., and Cheng, T. (2010). Q's next: the diverse functions of glutamine in metabolism, cell biology and cancer. Oncogene 29, 313-24.

Düvel, K., Yecies, J.L., Menon, S., Raman, P., Lipovsky, A.I., Souza, A.L., Triantafellow, E., Ma, Q., Gorski, R., Cleaver, S., et al. (2010). Activation of a metabolic gene regulatory network downstream of mTOR complex 1. Mol. Cell 39, 171-83.

Mellinghoff, I.K., Wang, M.Y., Vivanco, I., Haas-Kogan, D.A., Zhu, S., Dia, E.Q., Lu, K.V., Yoshimoto, K., Huang, J.H., Chute, D.J., et al. (2005). Molecular determinants of the response of glioblastomas to EGFR kinase inhibitors. N. Engl. J. Med. 353, 2012-24.

McFate, T., Mohyeldin, A., Lu, H., Thakar, J., Henriques, J., Halim, N.D., Wu, H., Schell, M.J., Tsang, T.M., Teahan, O., et al. (2008). Pyruvate dehydrogenase complex activity controls metabolic and malignant phenotype in cancer cells. J. Biol. Chem. 283, 22700-8.

Spiegel, S., Milstien, S., and Grant, S. (2012). Endogenous modulators and pharmacological inhibitors of histone deacetylases in cancer therapy. Oncogene 31, 537-51.

Yang, X.J., and Seto, E. (2007). HATs and HDACs: from structure, function and regulation to novel strategies for therapy and prevention. Oncogene 26, 5310-8.